

## STIS Far UV Studies of Spatial and Temporal Activity Variations in YY Gem

S.H. Saar<sup>1</sup>, J.A. Bookbinder<sup>1</sup>

### Abstract.

We analyze STIS data of the eclipsing dM0e+dM0e system YY Gem, finding a spatially variable quiescent level, frequent and sometimes periodic flaring, and evidence for a spatially extended transition region.

### 1. Introduction, Observations, and Reduction

YY Gem is an eclipsing binary composed of spotted flare stars (M0Ve+ M0Ve) in a  $P_{\text{orb}} = 0.814$  day orbit. The system shows strong UV and X-ray (Haisch et al. 1990) emission. Doppler imaging reveals most spots located at mid-latitudes ( $\approx \pm 45^\circ$ ) with a smaller feature near the equator (Hatzes 1995). Coronal emission appears to be concentrated near the spots based on X-ray eclipse mapping (Güdel et al. 2001).

We have obtained HST time-tagged STIS data of YY Gem over 6 orbits. Scheduling difficulties forced us to relax our phase constraints, with the end result that only one of the six observations fell fully in the eclipse, and one partially. We corrected for time-step problems in the HST pipeline analysis, extracted and binned the data in time using software in the CIAO X-ray package. The resulting spectra were then analyzed with special purpose IDL software. We use the Haisch et al. ephemeris to phase the spectra.

### 2. Analysis and Results

All the major far UV lines are seen (Fig. 1 left), and in addition we detect many weaker lines, including some interesting high temperature species not detected previously (S III 1206Å; Fe XXI 1354Å; O V 1371Å; O III 1666Å). Fluxes in the stronger lines are generally consistent with previous IUE measurements (Haisch et al. 1990). Mean fluxes in eclipse (which lasts  $\Delta\phi \approx 0.1$  in phase) are somewhat enhanced in higher temperature lines (Si IV, C IV) relative to cooler species (Ly  $\alpha$ , O I, C II).

We identify the mean “quiescent” level for each line in each HST orbit by an analysis the photon count distribution  $N(C_\gamma)$  (Saar & Bookbinder 1998a; Silverman et al. 2001). We assume the lowest photon count bins represent emission from a “quiescent”, constant, purely random process, and fit these to a Poisson function, varying the number of bins fit to achieve the best reduced  $\chi^2$ .

---

<sup>1</sup>Harvard-Smithsonian Center for Astrophysics

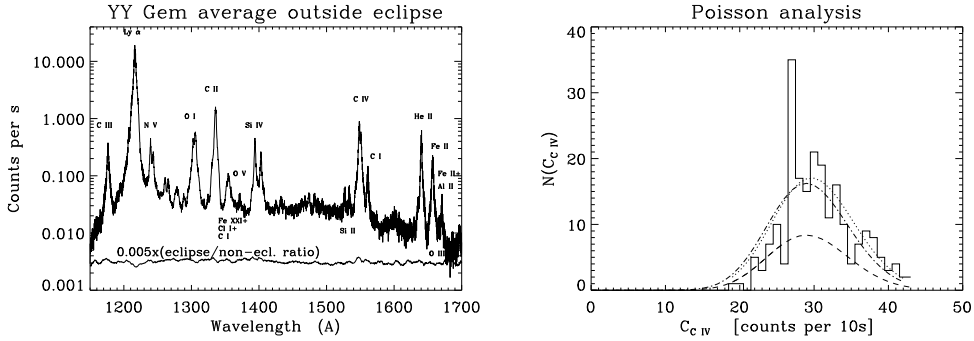


Figure 1. Left: The average STIS YY Gem spectrum outside of eclipse, with selected lines marked. A scaled ratio spectrum (average eclipse/average outside eclipse) is also plotted showing relative enhancements in TR lines (C IV, Si IV) and weakening in cooler lines (Ly  $\alpha$ , O I). Right: Analysis of the C IV timeseries in Fig. 3 left, showing the histogram of C IV counts ( $N(C_{\text{IV}})$ ; solid), a (poor) Poisson fit to the entire distribution (dotted;  $\chi^2_{\nu} = 30$ ), and a fit to the lowest portions of the distribution (dashed; the portion fit,  $19 \leq N(C_{\text{IV}}) \leq 25$  with  $\chi^2_{\nu} = 6.3$ , is in bold). The latter fit implies a maximum mean “quiescent” count rate of 29.4 counts/10 s (see dashed line; Fig. 3 left). Scaling this fit up to match the total number of detected counts yields an estimate of the maximum “flare-free”  $N_Q(C_{\text{IV}})$  (dot-dashed). The observed excess over this  $N_Q(C_{\text{IV}})$  indicates that *at least*  $\approx 4\%$  of the C IV flux derives from a non-Poisson (flare) process.

Since even these bins may be affected by low level flaring, the resulting Poisson fit represents an upper limit to the true distribution of quiescent photons unaffected by flaring. Scaling the amplitude of this Poisson fit until its integral matches the total number of observed photons yields an estimate of what the maximum quiescent distribution  $N_Q(C_{\gamma})$  would be in the absence of flaring. The excess of the observed  $N(C_{\gamma})$  over this maximum “flare-free” distribution then yields an estimate of the *minimum* distribution of photons from a non-Poisson (flare-like) process. An analysis of the C IV photon distribution for one HST orbit is shown in Figure 1 right.

The derived “quiescent” level (i.e., the Poisson mean of  $N_Q(C_{\gamma})$ ) – itself likely to be in part due to unresolved tiny flares – varies spatially over the stars, being strongest just outside secondary eclipse and weakest near primary eclipse (Fig. 2). Weak flares are a prominent feature in all the spectra, making analysis of underlying spatial structure difficult (cf. Saar & Bookbinder 1998b). Rapid semi-periodic flare spikes appearing in some time series (Fig. 3 left) are reminiscent of similar phenomena seen photometrically in other flare stars (e.g., Andrews 1990; Mullan et al. 1992). The Poisson analysis indicates that at least  $\sim 5\%$  of the flux in C IV can come from flares. Mullan et al. propose that the “periodic flares” may be due to oscillations in coronal loops.

Ingress into eclipse is more rapid, and eclipse is deeper, in chromospheric O I and C II compared to higher temperature transition region (=TR) lines Si

IV and C IV (Fig. 2). The similarity of the Si IV and C IV eclipses (Fig. 2) suggests that optical depth effects are probably not a significant cause of this effect; rather, the TR may be spatially extended by  $\approx 0.01$  in  $\phi$  ( $\approx 0.2R_*$ ) near the eclipsed limb (Fig. 3 right). Some caution is needed: since one set of observations were taken two days after the first, active region evolution may have taken place (as seen in CM Dra M4Ve+M4Ve; Saar & Bookbinder 1998b). Such evolution though would require a  $\sim 20\%$  drop in the chromospheric emission with no parallel change in the TR. The effect seems present at both primary and secondary eclipses though, which argues more in favor of a spatially extended TR.

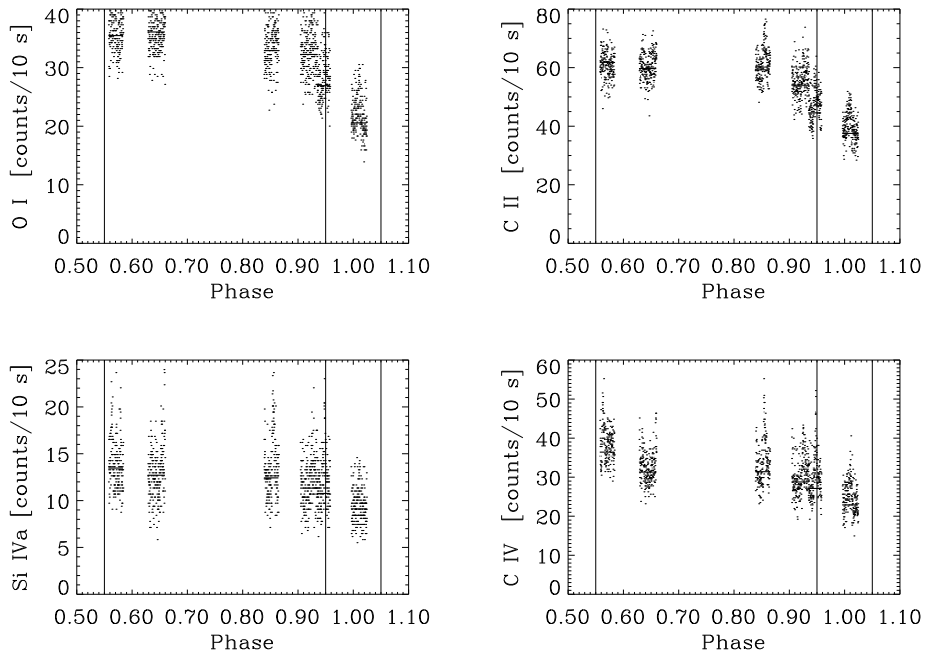


Figure 2. Counts per 10 s vs. orbital phase for four strong lines. The vertical lines delimit optical eclipses around  $\phi = 0.5$  and 1.0, while the horizontal lines give the quiescent (Poisson fit) mean for each orbit.

**Acknowledgments.** This research was funded by HST Grant GO-7440.

## References

- Andrews, A.D. 1990, *A&A*, 227, 456  
 Güdel, M. et al. 2001, *A&A*, 365, L344  
 Hatzes, A.P. 1995, in *IAU 176, Stellar Surface Structure (Poster Volume)*, ed. K. Strassmeier, Vienna, 90  
 Haisch, B.M., Schmitt, J.H.M.M., Rodonó, M., & Gibson, D.M. 1990, *A&A*, 230, 419

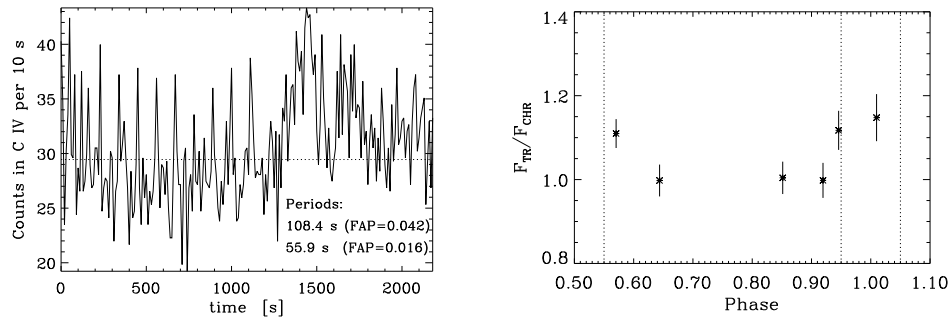


Figure 3. Left: Time series centered at phase  $\phi \sim 0.92$  studied in Fig. 1 right (the estimated quiescent mean from the Poisson analysis is dashed) showing quasi-periodic flare spikes. Periodogram analysis yields two periods (the shorter one may be a harmonic of the longer) with the given false alarm probabilities (FAP). Similar periods have been seen in optical photometry of some flare stars. Right: Ratios of mean quiescent counts in TR lines (C IV + Si IV + N V) relative to chromospheric lines (C II + O I), rescaled to average value well outside of eclipses. Note that the TR lines are enhanced relative to the cooler lines just outside of eclipses (delimited by vertical lines), suggesting that the TR emission may be spatially extended.

- Mullan, D.J., Herr, R.B., & Bhattacharyya, S. 1992, ApJ, 391, 265  
 Saar, S.H., Bookbinder, J.A. 1998a, in ASP Conf. Ser. 154, Cool Stars, Stellar Systems and the Sun, eds. J.A. Bookbinder & R.A. Donahue (San Francisco: ASP), CD-1560  
 Saar, S.H., Bookbinder, J.A. 1998b, *ibid*, CD-2042  
 Silverman, J.D., Eriksen, K., Green, P., & Saar, S.H. 2001, MNRAS, 323, 577